Resource

Cell Host & Microbe

An Infectious cDNA Clone of Zika Virus to Study Viral Virulence, Mosquito Transmission, and Antiviral Inhibitors

Graphical Abstract

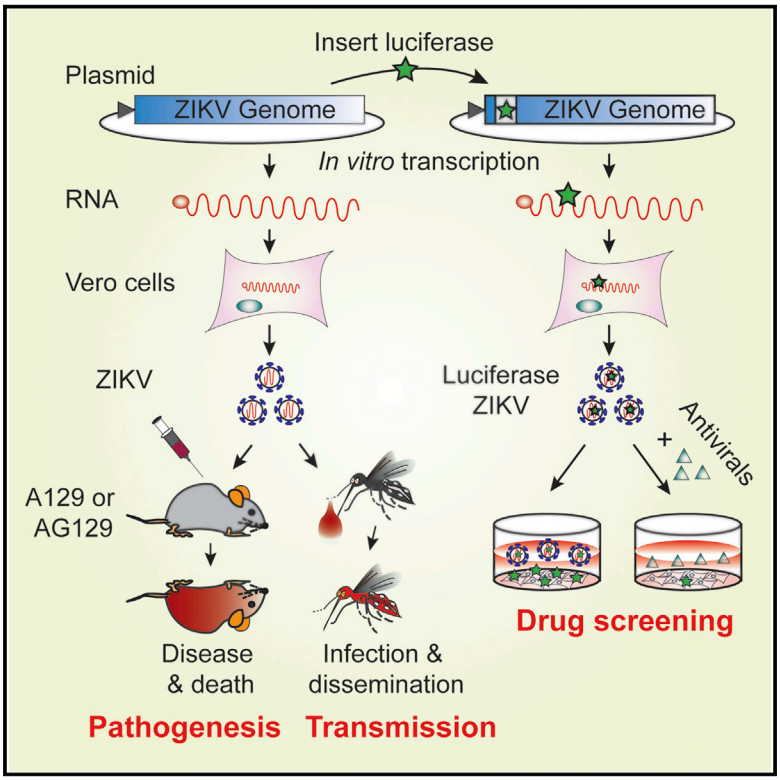

Highlights

- An infectious cDNA clone of Zika virus and a luciferase reporter virus were developed
- Recombinant Zika virus is virulent in A129 and AG129 mice
- Recombinant Zika virus is highly infectious for *Aedes aegypti* mosquitos
- The luciferase Zika virus can be used for antiviral drug discovery

Authors

Chao Shan, Xuping Xie, Antonio E. Muruato, ..., Nikos Vasilakis, Scott C. Weaver, Pei-Yong Shi

Correspondence

peshi@utmb.edu

In Brief

Zika virus (ZIKV) is causing devastating epidemics with severe disease. Shan et al. generated an infectious cDNA clone of ZIKV as well as a luciferase reporter virus. Recombinant ZIKV is virulent in mice and infectious in *Aedes aegypti* and thus may help identify viral determinants of virulence and transmission.

Shan et al., 2016, Cell Host & Microbe *19*, 1–10
June 8, 2016
http://dx.doi.org/10.1016/j.chom.2016.05.004

CellPress

Please cite this article in press as: Shan et al., An Infectious cDNA Clone of Zika Virus to Study Viral Virulence, Mosquito Transmission, and Antiviral Inhibitors, Cell Host & Microbe (2016), http://dx.doi.org/10.1016/j.chom.2016.05.004

Cell Host & Microbe
Resource

An Infectious cDNA Clone of Zika Virus to Study Viral Virulence, Mosquito Transmission, and Antiviral Inhibitors

Chao Shan,[1] Xuping Xie,[1] Antonio E. Muruato,[2,3] Shannan L. Rossi,[2,4] Christopher M. Roundy,[2,3] Sasha R. Azar,[2,3] Yujiao Yang,[1] Robert B. Tesh,[2,4] Nigel Bourne,[5,6,7] Alan D. Barrett,[2,4,6] Nikos Vasilakis,[2,4] Scott C. Weaver,[2,3,5,6,8] and Pei-Yong Shi[1,8,9,*]

[1]Department of Biochemistry and Molecular Biology
[2]Institute for Human Infections and Immunity
[3]Institute for Translational Science
[4]Department of Pathology and Center for Biodefense and Emerging Infectious Diseases
[5]Department of Microbiology and Immunology
[6]Sealy Center for Vaccine Development
[7]Department of Pediatrics
[8]Department of Pharmacology and Toxicology
[9]Sealy Center for Structural Biology and Molecular Biophysics
University of Texas Medical Branch, Galveston, TX 77555, USA
*Correspondence: peshi@utmb.edu
http://dx.doi.org/10.1016/j.chom.2016.05.004

SUMMARY

The Asian lineage of Zika virus (ZIKV) has recently caused epidemics and severe disease. Unraveling the mechanisms causing increased viral transmissibility and disease severity requires experimental systems. We report an infectious cDNA clone of ZIKV that was generated using a clinical isolate of the Asian lineage. The cDNA clone-derived RNA is infectious in cells, generating recombinant ZIKV. The recombinant virus is virulent in established ZIKV mouse models, leading to neurological signs relevant to human disease. Additionally, recombinant ZIKV is infectious for *Aedes aegypti* and thus provides a means to examine virus transmission. The infectious cDNA clone was further used to generate a luciferase ZIKV that exhibited sensitivity to a panflavivirus inhibitor, highlighting its potential utility for antiviral screening. This ZIKV reverse genetic system, together with mouse and mosquito infection models, may help identify viral determinants of human virulence and mosquito transmission as well as inform vaccine and therapeutic strategies.

INTRODUCTION

The current explosive epidemic of Zika virus (ZIKV) in the Americas poses a global public health emergency. ZIKV is a member of the *Flavivirus* genus within the *Flaviviradae* family. Flaviviruses have a positive-strand RNA genome of about 11,000 nucleotides. The flaviviral genome encodes three structural proteins (capsid [C], premembrane/membrane [prM/M], and envelope [E]) and seven nonstructural proteins (NS1, NS2A, NS2B, NS3, NS4A, NS4B, and NS5). The structural proteins form viral particles. The nonstructural proteins participate in viral replication, virion assembly, and evasion of the host immune response (Lindenbach et al., 2013). Like ZIKV, many flaviviruses are significant human pathogens, including yellow fever virus (YFV), West Nile virus (WNV), Japanese encephalitis virus (JEV), tick-borne encephalitis virus (TBEV), and dengue virus (DENV). ZIKV is transmitted by *Aedes* spp. mosquitoes, which also transmit YFV and DENV, as well as chikungunya virus (an emerging alphavirus). In addition, ZIKV may also be transmitted through sex, blood transfusion, and organ transplantation, and potentially through urine or saliva (Musso et al., 2014, 2015). Individuals with compromised immunity could be more susceptible to ZIKV infection and disease development (Shan et al., 2016).

Since its first isolation in Uganda in 1947 (Dick et al., 1952), ZIKV has predominantly been associated with sylvatic transmission cycles between primates and arboreal mosquitoes in forests and has for six decades rarely caused human diseases, with only 13 naturally acquired cases reported (Petersen et al., 2016). Up to 80% of infected people are asymptomatic. Signs and symptoms of ZIKV infection include fever, lethargy, conjunctivitis, rash, and arthralgia. However, in the past decade, ZIKV has emerged into urban transmission cycles between humans and mosquitoes in the South Pacific and the Americas, and has caused severe diseases, including Guillain-Barré syndrome and congenital microcephaly (Fauci and Morens, 2016). Phylogenetic analysis indicates ZIKV exists as African and Asian lineages. The Asian lineage is responsible for the recent/current epidemics: it caused an epidemic on Yap Island, Micronesia, in 2007; it then spread from an unknown source, probably in Southeast Asia, to French Polynesia and other regions of the South Pacific and caused large epidemics in 2013–2014; subsequently, ZIKV arrived in the Americas in 2015 and led to millions of human infections. It is currently not known what has triggered the surge of recent epidemics and severe diseases.

Experimental systems, including a reverse genetic system of ZIKV, animal models, and mosquito transmission models, are urgently needed to address these key scientific questions. For animal models, A129 (lacking interferon α/β receptors), AG129 (lacking interferon α/β and γ receptors), and *Irf3*$^{-/-}$ *Irf5*$^{-/-}$ *Irf7*$^{-/-}$ triple knockout mice were recently reported to be susceptible to ZIKV infection and to develop neurological diseases (Lazear et al., 2016; Rossi et al., 2016; Zmurko et al., 2016); infection of rhesus macaques with an Asian lineage ZIKV was also reported recently (Dudley et al., 2016). For mosquito infection, one study showed that *A. aegypti* and *A. albopictus* mosquitoes are unexpectedly poor vectors for ZIKV, with disseminated infection rates generally <50% following high-titer (10^7 tissue culture infectious dose 50%) oral doses. This suggests the possibility that other mosquito vectors or human-to-human transmission may be contributing to the explosive spread of the virus (Chouin-Carneiro et al., 2016).

Here we report the construction and characterization of a stable full-length cDNA clone of a clinical, Asian lineage ZIKV strain that could be used to make mutant viruses at any locations of the viral genome. The cDNA clone-derived ZIKV was virulent and caused neurological disease in A129 and AG129 mice. In addition, the recombinant virus was highly infectious for *A. aegypti* mosquitoes. Furthermore, the infectious cDNA clone could be used to generate a luciferase reporter ZIKV for antiviral drug discovery. These experimental systems are essential to study viral pathogenesis and vector transmission as well as to develop a ZIKV vaccine and therapeutics.

RESULTS

Construction of the Full-Length cDNA Clone of ZIKV

We chose a clinical ZIKV isolate of Asian lineage to construct the cDNA clone. This ZIKV strain (FSS13025) was isolated from a 3-year-old patient from Cambodia in 2010 (Heang et al., 2012). Viral RNA from Vero cell passage two of the isolate was sequenced (GenBank number KU955593.1) and used as the template to construct the infectious cDNA clone. Five RT-PCR fragments (A–E) spanning the complete viral genome were individually cloned and assembled into the full-length cDNA of ZIKV (named as pFLZIKV; Figure 1A). Based on our previous experience with infectious clones of other flaviviruses (Li et al., 2014; Shi et al., 2002; Zou et al., 2011), we chose a low-copy number plasmid pACYC177 (15 copies per *E. coli* cell) to clone fragments A and B as well as to assemble the full-genome cDNA. This plasmid was used because fragments A and B, spanning the viral prM-E-NS1 genes, were toxic to *E. coli* during the cloning procedure; high copy-number vectors containing these fragments were unstable, leading to aberrant deletions/mutations of the inserts (Shi et al., 2002). In contrast, fragments C, D, and E were not toxic to *E. coli* and could be cloned individually into a high copy-number plasmid pCR2.1-TOPO. A T7 promoter and a hepatitis delta virus ribozyme (HDVr) sequence were engineered at the 5′ and 3′ ends of the complete viral cDNA for in vitro transcription and for generation of the authentic 3′ end of the RNA transcript, respectively. Sequence comparison of the fully assembled pFLZIKV cDNA with the parental virus revealed two synonymous mutations in the E gene (Table 1), one of which was derived from an engineered genetic marker (see below). The complete DNA sequence of pFLZIKV is shown in Supplemental Experimental Procedures, available online. RNA synthesized from the pFLZIKV plasmid (10,807 nt long without HDVr) and RNA transcribed from a DENV-2 infectious clone (10,723 nt long; Zou et al., 2011) migrated similarly on a native agarose gel (Figure 1B).

RNA Transcript from ZIKV cDNA Clone Is Infectious

We transfected the pFLZIKV RNA transcript into Vero cells to examine the infectivity of the cDNA clone. The transfected cells were monitored for viral protein expression, RNA synthesis, and virus production. As shown in Figure 1C, an increasing number of cells expressed viral E protein from day 3 to day 6 post-transfection (p.t.). RT-PCR analysis detected ZIKV RNA in culture media of the transfected cells; as a negative control, no RT-PCR product was detected from the cells transfected with an RNA containing the polymerase active site GDD residues mutated to AAA (Figure 1D). Increasing amounts of infectious virus were produced from the wild-type RNA-transfected cells, with peak titers of $1 \times 10^{6-7}$ plaque-forming units (PFUs)/ml on days 5–7 (Figure 1E). On days 6–7 p.t., the transfected cells exhibited cytopathic effects (CPE; Figure 1F). Full-genome sequencing of the recombinant virus revealed no change other than the two synonymous mutations that originated from pFLZIKV. Collectively, these results demonstrate that the ZIKV cDNA clone is infectious.

Comparison of Cell Culture Growth between Parental and Recombinant Viruses

We compared the recombinant and parental viruses in cell culture. As shown in Figure 2A, the recombinant virus produced homogeneous plaque morphology, whereas the parental virus generated heterogeneous plaque sizes. The difference in plaque morphology was not surprising, because the recombinant viruses were derived from a homogenous population of RNA transcripts, whereas the parental virus presumably was composed of a quasispecies. In agreement with this notion, the recombinant virus displayed attenuated replication kinetics in both mammalian Vero and mosquito C6/36 cells (Figures 2B and 2C), indicating that the replication level of recombinant virus was attenuated in cell culture.

Recombinant ZIKV Retained an Engineered Genetic Marker

To exclude the possibility that the recovered recombinant virus represented contamination with the parental virus, we engineered a genetic marker into the recombinant virus, in which an *SphI* cleavage site in the E gene from the parental virus was eliminated (Figure 2D). A 1,250 bp fragment spanning nucleotides 1,303–2,552 of viral genome was amplified using RT-PCR from RNAs extracted from the parental and recombinant viruses. The RT-PCR product from the parental virus was readily cleaved by *SphI*, whereas the RT-PCR product from the recombinant virus was resistant to *SphI* digestion (Figure 2E). These results demonstrate that the recombinant virus was produced from the cDNA-derived RNA transcript. The genetic marker allows differentiation and quantification between the recombinant virus and potentially other ZIKV isolates (which have

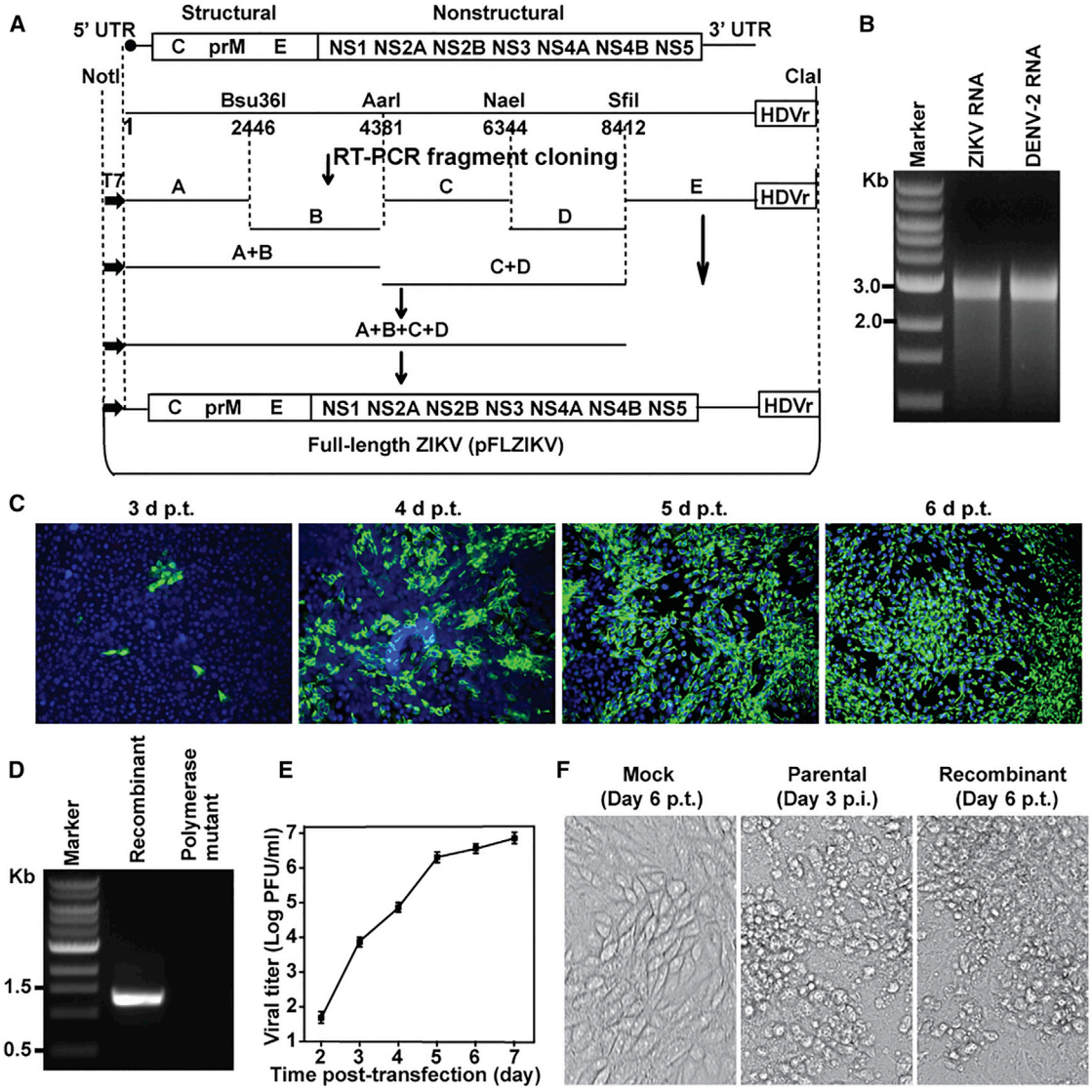

Figure 1. Construction of the Infectious cDNA Clone of ZIKV

(A) The strategy for constructing the full-length cDNA clone of ZIKV. Genome organization, unique restriction sites, and their nucleotide positions are shown. Five cDNA fragments from A to E (represented by thick lines) were synthesized from genomic RNA using RT-PCR to cover the complete ZIKV genome. Individual fragments were assembled to form the full-length cDNA clone of ZIKV (pFLZIKV). The complete ZIKV cDNA is positioned under the control of T7 promoter elements for in vitro transcription. An HDVr ribozyme sequence was engineered at the 3′ end of viral genome to generate an authentic 3′ end of viral RNA sequence. The numbers are the nucleotide positions based on the sequence of ZIKV strain FSS13025 (GenBank: KU955593.1).

(B) Analysis of RNA transcript from pFLZIKV on a native agarose gel. A 0.8% agarose gel electrophoresis was used to analyze ZIKV RNA transcript along with a genome-length DENV-2 RNA.

(C) IFA of viral protein expression in cells transfected with full-length ZIKV RNA. Vero cells were electroporated with 10 μg of genome-length ZIKV RNA. From day 3 to day 6 p.t., IFA was performed to examine viral E protein expression using a mouse mAb (4G2). Green and blue represent E protein and nuclei (stained with DAPI), respectively.

(D) RT-PCR analysis of progeny viral RNA. Viral RNA was extracted from culture supernatant on day 6 p.t. and used as a template for RT-PCR using ZIKV-specific primer pair 1303-F and 2552-ClaI-R (Table S2). As a negative control, a genome-length RNA containing an NS5 polymerase active site mutation (GDD mutated to AAA) was included.

(E) Yield of infectious ZIKV after transfection. Viral titers from culture supernatants at indicated time points were determined by plaque assay.

(F) Cytopathic effect (CPE) on Vero cells on day 6 p.t. CPE of Vero cells infected with parental virus on day 3 p.i. is included as a positive control.

the *SphI* site); it could be used to study viral fitness when the recombinant virus serves as an internal standard to gauge viral fitness of other ZIKV strains in a competition assay (Fitzpatrick et al., 2010).

The Infectious cDNA Clone of ZIKV Is Stable

Since infectious cDNA clones of flaviviruses are known to be unstable and deleterious for bacterial host (Khromykh and Westaway, 1994; Lai et al., 1991; Mandl et al., 1997; Rice et al., 1989;

Table 1. Sequence Differences between the Infectious cDNA Clone and Parental ZIKV

Nucleotide Position	Parental Strain	cDNA Clone	Amino Acid Change	Location
1,655	T	C	Silent (*SphI* knockout)	E
1,865	T	C	None	E

ZIKV strain FSS13025 (GenBank: KU955593.1) was used in the current study.

Sumiyoshi et al., 1992), we examined the stability of pFLZIKV through five rounds of plasmid transformation, bacterial growth, and plasmid purification. Plasmid purified from round five was used to transcribe RNA for an infectivity testing. Transfection of the fifth round RNA into Vero cells generated viral E protein-expressing cells (Figure S1A) and infectious virus (Figure S1B) at levels equivalent to those derived from the original pFLZIKV RNA without passaging (Figures S1A and S1B). Similar plaque morphology was observed for the original and fifth-round RNA-derived recombinant viruses (Figure S1C). These results demonstrate the stability of the ZIKV infectious clone.

Virulence in A129 and AG129 Mice

We compared the virulence of the parental and recombinant ZIKVs in two mouse models: A129 (lacking interferon α/β receptor) and AG129 (lacking interferon α/β and γ receptors). The AG129 mice have recently been reported to be more susceptible to ZIKV-induced disease than the A129 mice (Rossi et al., 2016). In the A129 mice, intraperitoneal (i.p.) infection with parental virus (10^5 PFU) led to weight loss and disease characterized by hunched posture and ruffled fur; all infected mice were euthanized due to >20% weight loss on day 9 post-infection (p.i.; Figure 3A). In contrast, infection with the same inoculum of recombinant ZIKV resulted in less weight loss, but none of the infected mice died (Figure 3A). In agreement with these observations, the recombinant virus generated significantly lower viremia than the parental virus on day 1 p.i. in the A129 mice, whereas the differences on day 2 and 3 viremia were not statistically significant between the two viruses (Figure 3B). The results suggest that the slower replication kinetics of the recombinant virus may be responsible for its attenuated virulence.

In AG129 mice, i.p. injection of both parental and recombinant ZIKVs ($1 \times 10^{3-5}$ PFU) led to neurological disease, weight loss, and death (due to >20% weight loss; Figure 4). The neurological disease was characterized by hyperactivity, uncoordinated movements, inability to right the body, body spinning, and hindlimb paralysis. The kinetics of weight loss was dependent on the viral dose: mice infected with the recombinant virus exhibited slower weight loss and longer survival than those infected with the parental virus (Figure 4). These results demonstrate that the recombinant virus is less virulent than the parental virus in vivo; however, infection of AG129 mice with the recombinant virus still leads to neurological disease. Therefore, the infectious cDNA clone could be used for mutagenesis analysis to identify potential viral virulent determinants.

Mosquito Infection and Dissemination

To compare viral fitness between parental and recombinant viruses in mosquitoes, we determined the oral susceptibility of *A. aegypti* using artificial human blood meals containing ZIKV. On day 14 post-feeding, engorged mosquitos were analyzed for the presence of virus in the bodies and legs to indicate viral infection rate and dissemination rate, respectively. As summarized in Table 2, the recombinant virus showed higher infection and disseminated infection rates than the parental virus, which may have reflected the slightly higher blood meal titer of the recombinant virus. The overall dissemination rates (number of disseminated mosquitoes / number of infected mosquitoes × 100%) were equivalent between the parental and recombinant viruses, suggesting that the recombinant virus has a wild-type phenotype in *A. aegypti* mosquitoes. These results demonstrate that the recombinant virus is highly infectious for *A. aegypti*, and the disseminated infection rates suggest that this species is an efficient vector for ZIKV.

A Luciferase Reporter ZIKV for Antiviral Drug Discovery

To demonstrate the utility of the reverse genetic system, we engineered a *Renilla* luciferase (Rluc) gene into the infectious cDNA clone. The *Rluc* gene was inserted at the viral capsid coding sequence (Figure 5A), as previously reported for YFV (Shustov et al., 2007). Transfection of the genome-length Rluc ZIKV RNA into Vero cells generated robust luciferase signals (Figure S2A). Infection of Vero cells using culture medium from the transfected cells produced luciferase activities (Figure S2B), indicating that infectious reporter ZIKV had been produced. The reporter virus could not be detected using plaque assay (even after incubating the infected cells for 6 days p.i.; data not shown) but could be clearly detected using an immunostaining focus assay (Figure 5B), indicating that insertion of the luciferase gene attenuated viral replication.

Using a known panflavivirus inhibitor (nucleoside analog NITD008; Lo et al., 2016; Yin et al., 2006), we examined whether the reporter ZIKV could be used for antiviral testing. As shown in Figure 5C, treatment of Rluc ZIKV-infected cells with NITD008 exhibited a dose-dependent inhibition of the luciferase signals; the luciferase inhibition suggested an EC_{50} value of 2.5 μM. No cytotoxicity was observed up to 100 μM of the inhibitor (Figure 5C). To validate the antiviral activity derived from the reporter virus, we performed viral titer reduction assay to estimate the compound efficacy against wild-type ZIKV (Figure 5D). The viral titer reduction results suggested an EC_{50} value of 3.6 μM, which is comparable to the EC_{50} value derived from the reporter virus system. Collectively, the results demonstrate that a luciferase reporter ZIKV could be used for antiviral drug screening.

DISCUSSION

Our reverse genetic system, together with the mosquito infection and A129/AG129 mouse models, provide a tractable platform to explore the mechanisms responsible for the explosive epidemics and increased disease severity of ZIKV infection since 2007. A number of nonexclusive mechanisms are possible. (1) ZIKV has undergone adaptive evolution that enhanced mosquito transmission, leading to rapid virus spread and an increased number of human infections. This hypothesis could be tested by comparisons of mosquito infectivity of the older ZIKV strains with recent isolates, followed by using the reverse genetic system to test the effects of recent mutations

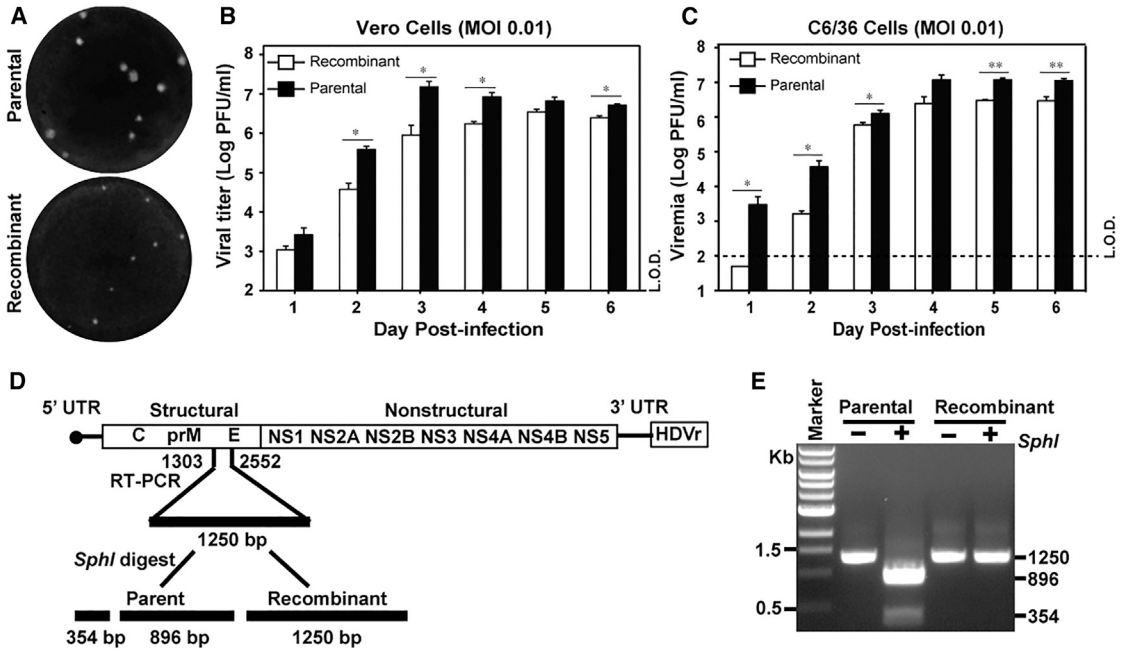

Figure 2. Characterization of Parental and Recombinant ZIKVs in Cell Culture

(A) Plaque morphology of parental and recombinant ZIKVs.

(B and C) Comparison of growth kinetics in Vero and C6/36 cells, respectively. Vero and C3/36 cells were infected with parental and recombinant virus at an MOI of 0.01. Viral titers were measured at indicated time points using plaque assays on Vero cells. Means and SDs from three independent replicates are shown. Statistics were performed using unpaired Student's t test; *significant ($p < 0.05$); **highly significant ($p < 0.01$). L.O.D., limitation of detection (100 PFU/ml).

(D) An engineered genetic marker in the recombinant ZIKV. An *SphI* cleavage site, located in the viral E gene of parental virus, was knocked out in the cDNA clone to serve as a genetic marker to distinguish between recombinant virus and parental virus. A 1,250 bp fragment (from nucleotides 1,303 to 2,552) spanning the *SphI* site was amplified using RT-PCR from RNA extracted from either recombinant virus or parental virus. The RT-PCR fragments were subjected to *SphI* digestion. The 1,250 bp fragment derived from recombinant virus should not be cleavable by *SphI*, whereas the RT-PCR fragment amplified from parental viral RNA should be cleavable by *SphI*. The expected sizes of the digestion products are indicated.

(E) Agarose gel analysis of *SphI* digestion products. Expected digestion pattern observed as depicted in (D) was observed. The lengths of DNA fragments are indicated on the right side of the agarose gel.

on mosquito transmission. This mechanism was responsible for the emergence of Chikungunya virus, in which a series of mutations in the viral envelope genes enhanced viral transmission by *A. albopictus* through increased infection of epithelial cells in the midgut (Tsetsarkin et al., 2014; Tsetsarkin and Weaver, 2011). (2) The Asian lineage of ZIKV has adapted to generate higher viremia in humans, leading to enhanced crossplacental infection and microcephaly. This hypothesis could be tested by engineering adaptive mutations from the recent isolates into the infectious cDNA clone, generating mutant viruses, and quantifying the mutational effect on viral virulence in the A129/AG129 mouse and on microcephaly development. (3) Stochastic introduction of ZIKV into a population (in the Pacific and Americas) lacking herd immunity led to greater susceptibility to ZIKV infection and efficient mosquito transmission. Seroprevalence and its correlation with ZIKV transmission and outbreak frequency

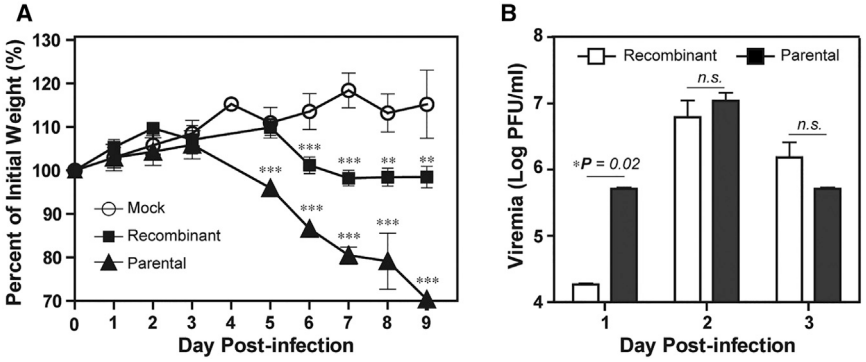

Figure 3. Comparison of Virulence in A129 Mice between Recombinant and Parental Viruses

Four-week-old A129 mice were infected with 1×10^5 PFU per individual via the intraperitoneal route. Mock or infected mice (n = 5 per group) were monitored for weight loss (A). The viremia at the first 3 days p.i. was quantified using plaque assay (B). Means and SDs are shown. One-way ANOVA test was performed to evaluate the statistical significance of weight differences among the mock-infected, parental virus-infected, and recombinant virus-infected mice. The unpaired Student's t test was performed to estimate the viremia differences in mice infected with recombinant and parental viruses; *significant ($p < 0.05$); **very significant ($p < 0.01$); ***extremely significant ($p < 0.001$).

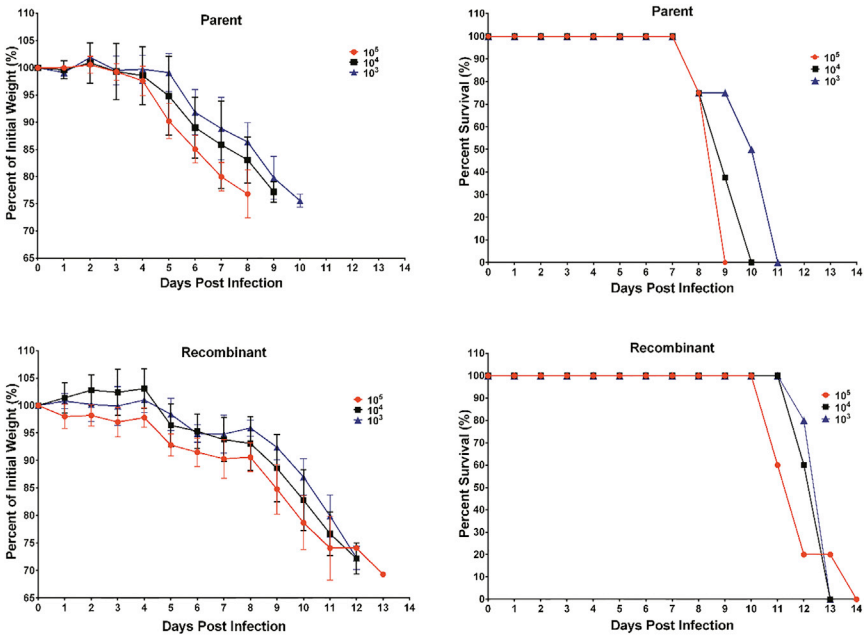

Figure 4. Virulence of Parental and Recombinant ZIKVs in AG129 Mice

Six-week-old AG129 mice were inoculated by intraperitoneal injection with 1×10^5 PFU (n = 4 for parental virus; n = 5 for recombinant virus), 1×10^4 PFU (n = 8 for parental virus; n = 5 for recombinant virus), or 1×10^3 PFU (n = 4 for parental virus; n = 5 for recombinant virus) of ZIKV. The infected mice were monitored for weight loss. Mice were euthanized once weight loss exceeded >20%. For each infection dose, weight loss and survival curves are presented. Parental and recombinant viruses and their infection doses are indicated. Values are mean percent weight compared to initial weight.

need to be established to address this hypothesis. (4) Previous infection with DENV may exacerbate ZIKV disease severity because the two viruses share high amino acids identity and extensive antibody crossreactivity (Alkan et al., 2015; Lanciotti et al., 2008). This hypothesis could be tested in the AG129 mouse because this mouse is susceptible to both DENV and ZIKV infections. (5) Human genetic predisposition may account for the severe disease outcomes. Any viral infection is modulated by proviral and antiviral host factors. The interaction between viral and host factors determines the efficiency of infection, pathogenicity, transmission, and epidemic potential. Therefore, variations of critical host factor(s) among infected individuals may contribute to different disease severity.

Compared with the parental virus, the replication efficiency of the recombinant virus was reduced in Vero and C6/36 cells (Figure 2). This attenuated replication of recombinant virus in Vero cells was translated to the attenuated virulence in the A129 and AG129 mice (Figures 3 and 4). The differences (in replication and virulence) between the parental and recombinant viruses might be due to the limited genetic heterogeneity of the recombinant virus population and the more genetically diverse quasispecies nature of the parental virus. It should be noted that an alternative infectious cloning approach could be used to generate quasispecies of virus that reflect parental virus population (Edmonds et al., 2013; Siridechadilok et al., 2013); the virulence of the viruses derived from the two infectious cloning approaches (the alternative approach and the current approach described in this study) could be compared in the AG129 mouse model. For mosquito experiments, although the replication of the recombinant virus was reduced in C6/36 cells, it yielded a disseminated infection rate in *A. aegypti* mosquitoes similar to that of the parental virus, indicating that the cell culture system does not necessarily recapitulate in vivo outcomes. Such a discrepancy is not surprising because of the more complex host-virus interactions in vivo.

The infectious cDNA clone of ZIKV will facilitate vaccine development through rational design. Target-based attenuation of ZIKV could be achieved through mutating viral replication components (viral RNA and replication complex) or through ablating viral components needed for evasion of host immune response (Li et al., 2013; Whitehead et al., 2007; Züst et al., 2013). The ZIKV strain used in the current study is appropriate for such attenuated vaccine because of its high sequence similarity to the American epidemic strains. As summarized in Table S1, only 19 amino acid differences were observed between our infectious clone-derived virus and strains recently isolated from microcephaly fetuses (Calvet et al., 2016; Faria et al., 2016; Mlakar et al., 2016), representing >99% amino acid identity. In addition, the recombinant virus was attenuated in both A129 and AG129 mice yet replicated robustly in Vero cells (an approved cell line for vaccine production) to titers above 1×10^6 PFU/ml. Besides its application for vaccine development, the infectious clone could also be used to generate reporter ZIKV, which would facilitate the tracking of viral replication in vivo and screening for antiviral inhibitors in a high-throughput manner (Shan et al., 2016). Indeed, we showed that a luciferase reporter ZIKV could be generated; such a reporter virus could be used for antiviral drug screening.

In summary, the current study has provided a multicomponent platform to study ZIKV transmission and disease pathogenesis and to develop countermeasures.

EXPERIMENTAL PROCEDURES

Cells, Viruses, and Antibodies

Vero cells were purchased from the American Type Culture Collection (ATCC, Bethesda, MD), and maintained in a high-glucose Dulbecco's modified Eagle's medium (DMEM) (Invitrogen, Carlsbad, CA) supplemented with 10% fetal bovine serum (FBS) (HyClone Laboratories, Logan, UT) and 1% penicillin/streptomycin (Invitrogen) at 37°C with 5% CO_2. *A. albopictus* C6/36 (C6/36) cells were grown in RPMI1640 (Invitrogen) containing 10% FBS and 1% penicillin/streptomycin at 28°C with 5% CO_2. The parental ZIKV Cambodian strain FSS13025 (GenBank number KU955593.1) was isolated in 2010 from the blood of a patient from Cambodia. The following antibodies were used in this study: a mouse monoclonal antibody (mAb) 4G2 crossreactive with flavivirus E protein (ATCC) and goat anti-mouse IgG conjugated with Alexa Fluor 488 (Thermo Fisher Scientific).

Table 2. Infection and Dissemination of Asian Lineage ZIKV Strain FSS13025 in *A. aegypti*

Strain	Blood Meal Titer (Log_{10} FFU/ml)[a]	Infection Rate (%)[b]	Disseminated Infection Rate (%)[c]	Dissemination Rate (%)[d]
FSS13025 parental	6.2	18/42 (43)	11/42 (26)	11/18 (61)
FSS13025 recombinant	6.5	33/42 (78)	19/42 (45)	19/33 (58)

[a]After blood meal, viral titers for both parental and recombinant viruses were measured by focus-forming assay to ensure the accuracy of virus amounts in the blood meal.
[b]Infection rate = number of infected mosquitos / number of engorged mosquitos × 100%.
[c]Disseminated infection rate = number of disseminated mosquitos / number of engorged mosquitos × 100%.
[d]Dissemination rate (%) = number of disseminated mosquitos / number of infected mosquitos × 100%.

cDNA Synthesis and Cloning

Viral RNA from Vero cell passage two of ZIKV Cambodian strain FSS13025 was sequenced. Specifically, viral RNA was extracted from viral stocks using QIAamp Viral RNA Kits (QIAGEN). cDNA fragments covering the complete genome were synthesized from genomic RNA using SuperScript III (RT)-PCR using primers (Table S2) according to the manufacturer's instructions (Invitrogen). Figure 1A depicts the scheme to clone and assemble the full genome of ZIKV. Plasmid pACYC177 (New England Biolabs, Ipswich, MA) was used to clone fragments B and A+B. Plasmid pCR2.1-TOPO (Invitrogen) was used to clone individual fragments C, D, and E. The full-length genomic cDNA was assembled using plasmid pACYC177. Bacterial strain Top 10 (Invitrogen) was used as the *E. coli* host for construction and propagation of cDNA clones. A standard cloning procedure was used, as previously reported for making WNV (Shi et al., 2002) and DENV (Zou et al., 2011) infectious clones. The virus-specific sequence of each intermediate clone was validated by Sanger DNA sequencing before it was used in subsequent cloning steps. The final plasmid containing full-length cDNA of ZIKV (pFLZIKV) was sequenced to ensure no undesired mutations. A T7 promoter and a HDVr sequence were engineered at the 5′ and 3′ ends of the complete viral cDNA using overlap RT-PCR for in vitro transcription and for generation of the authentic 3′ end of the RNA transcript, respectively. The All restriction endonucleases were purchased from New England Biolabs (Beverly, MA).

Construction of *Renilla* Luciferase Reporter Virus

An overlap cloning strategy was used to construct ZIKV-Rluc plasmid. First, a standard overlap PCR was used to create a cassette containing "NotI-T7 promoter-5′UTR-the first 25 amino acids of capsid protein-*Renilla* luciferase gene-FMDV 2A-authentic initiation codon of capsid protein to the unique AvrII site in E protein." Briefly, fragment A covering "NotI-T7 promoter-5′UTR-the first 25 amino acids" was amplified with the primers pACYC-14437-F and C25-Rluc-R using the pFLZIKV as a template. *Renilla* luciferase gene (fragment B) was amplified from Dengue-Rluc reporter virus by primers C25-Rluc-F and 2A-Cap-R. Fragment C spanning "the authentic initiation codon of capsid protein to AvrII unique site in E protein" (located at nucleotide position 1,533 of the viral genome) was amplified with primers 2A-Cap-F and 1818-R using the pFLZIKV as a template. Next, fragments A, B, and C were used to create cassette "NotI-T7 promoter-5′UTR-the first 25 amino acids of capsid protein-renilla luciferase gene-FMDV2A-authentic initiation codon of capsid protein to the unique AvrII site in E protein" by overlap PCR with primers pACYC-14437-F and 1818C. All primer sequences are listed in Table S2. Compared with the wild-type pFLZIKV, ZIKV-Rluc contained an extra fragment (representing the first 25 amino acids of C protein-a Renilla luciferase gene-FMDV2A) between the 5′UTR and the complete ORF of the viral genome. Silent mutations within the flavivirus-cyclization sequence (located in the amino acids 14–17 of the complete capsid gene) were engineered. All the constructs were verified by DNA sequencing.

RNA Transcription and Transfection

Plasmid pFLZIKV, containing the full-length cDNA of ZIKV, was amplified in *E. coli* Top10 and purified using MaxiPrep PLUS (QIAGEN). For in vitro transcription, 10 μg of pFLZIKV was linearized with restriction enzyme *ClaI*. The linearized plasmid was extracted with phenol-chloroform and chloroform, precipitated with ethanol, and resuspended in 15 μl of RNase-free water (Ambion, Austin, TX). The mMESSAGE mMACHINE kit (Ambion) was used to in vitro transcribe RNA in a 20 μl reaction with an additional 1 μl of 30 mM GTP solution. The reaction mixture was incubated at 37°C for 2 hr, followed by the addition of DNase I to remove the DNA template. The RNA was precipitated with lithium chloride, washed with 70% ethanol, resuspended in RNase-free water, quantitated by spectrophotometry, and stored at −80°C in aliquots. For transfection, approximately 10 μg of RNA was electroporated to 8×10^6 Vero cells in 0.8 ml of Ingenio Electroporation Solution (Mirus, Madison, WI), in 4 mm cuvettes with the GenePulser apparatus (Bio-Rad) at settings of 0.45 kV and 25 μF, pulsing three times, with 3 s intervals. After a 10 min recovery at room temperature, the transfected cells were mixed with media and incubated in a T-175 flask (5% CO_2 at 37°C). At different time points p.t., recombinant viruses in cell culture media were harvested, clarified by centrifugation at 500 × g, stored in aliquots at −80°C, and subjected to analysis.

Indirect Immunofluorescence Assays

Indirect immunofluorescence assay (IFA) was performed to detect viral protein expression in ZIKV RNA-transfected Vero cells. Vero cells transfected with viral RNA were grown in an 8-well Lab-Tek chamber slide (Thermo Fisher Scientific, Waltham, MA). At indicated time points, the cells were fixed in 100% methanol at −20°C for 15 min. After 1 hr incubation in a blocking buffer containing 1% FBS and 0.05% Tween-20 in PBS, the cells were treated with a mouse monoclonal antibody 4G2 for 1 hr and washed three times with PBS (5 min for each wash). The cells were then incubated with Alexa Fluor 488 goat anti-mouse IgG for 1 hr in blocking buffer, after which the cells were washed three times with PBS. The cells were mounted in a mounting medium with DAPI (4′, 6-diamidino-2-phenylindole; Vector Laboratories, Inc.). Fluorescence images were observed under a fluorescence microscope equipped with a video documentation system (Olympus).

Luciferase Assay

The Vero cells transfected with ZIKV-Rluc RNA (30 μg) were seeded in a 12-well plate. At various time points, the cells were washed once with PBS and lysed using cell lysis buffer (Promega). The cells were scraped from plates and stored at −80°C. Once samples for all time points had been collected, luciferase signals were measured in a luminescence microplate reader (PerkinElmer) according to the manufacturer's protocol.

Antiviral Assays

Two types of antiviral assays were performed: luciferase reporter ZIKV infection assay and wild-type ZIKV-based viral titer resection assay. For luciferase reporter ZIKV assay, Vero cells were seeded at 2×10^4 cells per well in 96-well plates. After incubation overnight, the cells were infected with the reporter virus at an MOI of 0.1 in the presence of compound NITD008. At 48 hr p.i., luciferase activity was measured using Enduren, and cell viability was estimated in an MTS assay as previously described (Wang et al., 2009). For viral titer reduction assay, Vero cells were infected with the recombinant wild-type ZIKV at an MOI of 0.05. The infected cells were treated with different concentrations of NITD008. At 48 hr p.i., the amount of infectious viruses in culture fluids was quantified using plaque assay on Vero cells. Compound NITD008 was generously provided by Novartis Institute for Tropical Diseases.

Restriction Enzyme Digestion Analysis to Differentiate between Parental and Recombinant Viruses

A restriction endonuclease site for *SphI* existing in the parental ZIKV was eliminated in the cDNA clone and the resulting recombinant virus. The

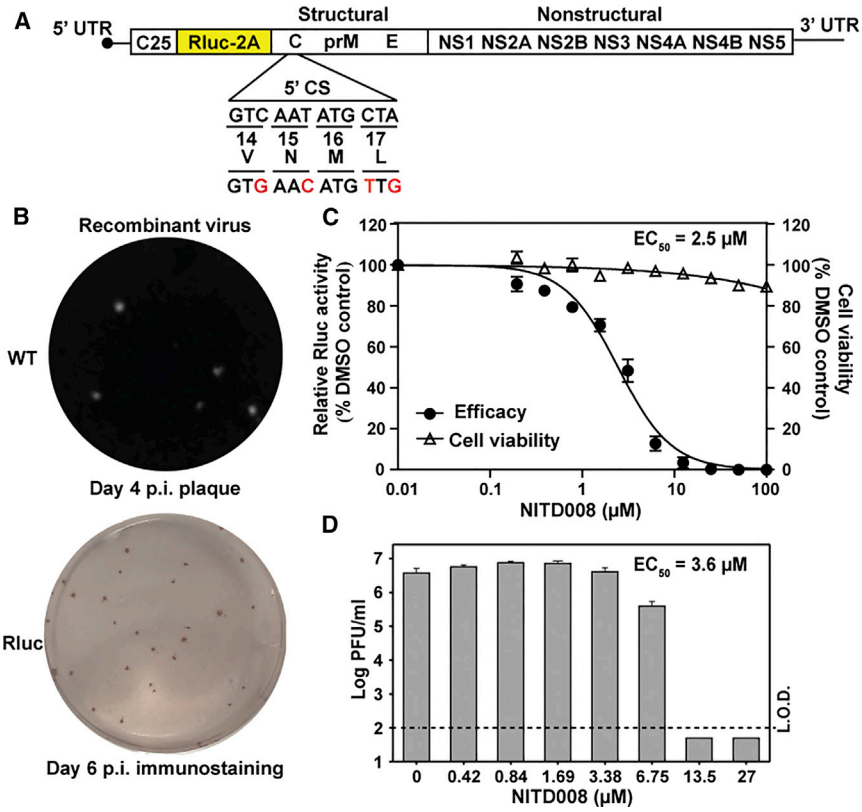

Figure 5. Construction of Reporter ZIKV for Antiviral Testing

(A) Construction of a *Renilla* luciferase (Rluc) reporter ZIKV. The luciferase gene was in-frame fused downstream of the first 25 amino acids of the vial capsid gene (indicated as "C25"); maintaining these 25 amino acids of capsid is essential for flavivirus genome cyclization required for viral replication. The 2A peptide from foot-and-mouth disease virus (indicated as "2A") was engineered between the C terminus of luciferase gene and the complete open reading frame of ZIKV; the 2A sequence enables cleavage between the C terminus of luciferase and the N terminus of the downstream capsid protein. Silent mutations within the flavivirus-cyclization sequence (located in amino acids 14–17 of the complete capsid gene) were engineered; the mutated nucleotides are indicated in red.

(B) Plaque morphology of the recombinant ZIKV and immunostaining foci of the Rluc ZIKV. Plaque assay was performed for the wild-type ZIKV on day 4 p.i. The Rluc ZIKV did not generate clear plaques (data not shown) but could be detected by immunostaining on day 6 p.i.

(C) Antiviral test using the reporter ZIKV. Vero cells were infected with the reporter ZIKV and treated with a panflavivirus nucleoside inhibitor NITD008 (Yin et al., 2009). At 48 hr p.i., the cells were measured for luciferase activities. An estimated EC_{50} value of 2.5 μM is indicated for NITD008.

(D) Anti-ZIKV activity of NITD008 using viral titer reduction assay. Vero cells were infected with wild-type ZIKV at an MOI of 0.05 in the presence of various concentrations of NITD008. At 48 hr p.i., viral titers in culture fluids were quantified using plaque assay. The viral titer reduction results suggest an EC_{50} value of 3.6 μM.

disappearance of the *SphI* site was used to distinguish between the parental (with *SphI* site) and recombinant (without *SphI* site) viruses. Recombinant virus (harvested from culture media on day 6 p.t.) and parental virus were subjected to RNA extraction using QIAamp Viral RNA Kits (QIAGEN). The extracted viral RNAs were used to amplify the 1,250 bp fragments spanning the *SphI* site using primers E-1303V and NS1-2552-ClaI-R (Table S2). The RT-PCR products were digested with *SphI* and analyzed on a 0.8% agarose gel.

Plaque Assay

Viral samples were 10-fold serially diluted six times in DMEM. For each dilution, 100 μl sample was added to a 12-well plate containing Vero cells at about 90% confluency. The infected cells were incubated for 1 hr and swirled every 15 min to ensure complete coverage of the monolayer for even infection. After the incubation, 1 ml of methyl cellulose overlay containing 5% FBS and 1% penicillin/streptomycin was added to each well, and the plate was incubated at 37°C for 4 days. Following the incubation, methyl cellulose overlay was removed; the plate was washed twice with PBS, fixed with 3.7% formaldehyde, and incubated at room temperature for 20 min. After removing the fixative, the plate was stained with 1% crystal violet for 1 min. Visible plaques were counted, and viral titers (PFU/ml) were calculated.

Replication Curves

Subconfluent Vero and C6/36 cells in 12-well plates were inoculated with either parental or recombinant ZIKV at an MOI of 0.01 in triplicate wells. Virus stocks were diluted in DMEM containing 5% FBS and 1% penicillin/streptomycin. One hundred microliters of virus was added to each well of the 12-well plates. After 1 hr attachment (5% CO_2 at 37°C for Vero cells and at 28°C for C6/36 cells), the inocula were removed. The cell monolayers were washed three times with PBS. Afterward, 1 ml DMEM medium containing 2% FBS and 1% penicillin/streptomycin was added to each well. The plates were incubated for up to 6 days. The medium was collected daily and subjected to plaque assay as described above.

Virulence in Mice

Both A129 and AG129 mice were used to examine the virulence of parental and recombinant ZIKVs. The details of parental ZIKV infection in A129 mice have been recently reported (Rossi et al., 2016). Briefly, 4-week-old A129 mice were infected with 1×10^5 PFU via the intraperitoneal route. Five mice per group were used for parental and recombinant viruses. PBS was used to dilute the virus stocks to the desired concentration. The inoculum was back-titrated to verify the viral dose. Mock-infected mice were given PBS by the same route. Mice were weighed and monitored daily for signs of illness (hunched posture, ruffled fur, lethargy, etc.). Mice were bled via the retro-orbital sinus (RO) after being anesthetized every other day. Blood was clarified post-collection by centrifugation at 3,380 × g for 5 min and immediately stored at −80°C for storage. Viral titers were determined by plaque assay on Vero cells. Mice were considered moribund if they did not respond to stimuli, were unable to remain upright, or lost 20% or more of their initial weight (consistent with the approved protocol).

The AG129 mice were bred and maintained in animal facilities at the University of Texas Medical Branch (UTMB). Young adult animals (6 weeks old) were inoculated by intraperitoneal injection with parental or recombinant ZIKV using a range of inocula. Following inoculation, mice were weighed daily and visually monitored to determine the course of infection. Mice exhibiting weight loss of >20% of initial body weight or neurologic disease were euthanized. Euthanized animals were counted as being dead on the following day for analysis. All animal work was completed in compliance with the UTMB policy as approved by the Institutional Animal Care and Use Committee (IACUC).

Experimental Infection of Mosquitoes with ZIKV

A. aegypti colony mosquitoes derived from Galveston, TX, were fed for 30 min on blood meals consisting of 1% (weight/vol) sucrose, 20% (vol/vol) FBS, 5 mM ATP, 33% (vol/vol) PBS-washed human blood cells (UTMB Blood Bank), and 33% (vol/vol) DMEM medium and combined with 1 ml virus offered in Hemotek 2-ml heated reservoirs (Discovery Workshops) covered with a mouse skin. Virus titer in the blood meals ranged from 6.2 to 6.5 $\log_{10}$ FFU/ml. Infectious blood meals were loaded on cartons containing *A. aegypti*. Engorged mosquitoes were incubated at 28°C, 80% relative humidity on a 12:12 hr light:dark cycle with ad libitum access to 10% sucrose solution for 14 days and then frozen at −20°C overnight. To assess infection and dissemination, bodies and legs were individually homogenized (Retsch MM300 homogenizer, Retsch Inc., Newton, PA) in DMEM with 20% FBS and 250 μg/ml amphotericin B. Samples were centrifuged for 10 min at 5,000 rpm, and 50 μl of each sample supernatant was inoculated into 96-well plates containing Vero cells at 37°C and 5% CO_2 for 3 days, when they were fixed with a mixture of ice-cold acetone and methanol (1:1) solution and immunostained as described below. Infection was determined by recovery of virus from the homogenized body, and dissemination from the alimentary track into the hemocoel was determined by recovery of virus from the legs. The infection rate was recorded as the fraction of virus-positive bodies divided by the total number of bodies from engorged mosquiteos, and the disseminated infection rate is the number of virus-positive legs divided by the total number of engorged mosquitoes.

Focus-Forming Assays and Immunostaining

Ten-fold serial dilutions of virus in DMEM supplemented with 2% FBS and 250 μg/ml amphotericin B (Invitrogen, Carlsbad, CA) were added onto confluent Vero cell monolayers attached to 96-well Costar (Corning, NY) plates and incubated for 1 hr with periodic gentle rocking to facilitate virus adsorption at 37°C. Wells were then overlaid with 150 μl of DMEM supplemented with 2% FBS and 250 μg/ml amphotericin B and incubated undisturbed for 3 days at 37°C. Media overlay was aspirated, and cell monolayers were rinsed once with PBS (pH 7.4) (Invitrogen, Carlsbad, CA), fixed with a mixture of ice-cold acetone and methanol (1:1) solution, and allowed to incubate for 30 min at room temperature. Fixation solution was aspirated, and plates were allowed to air dry. Plates were washed twice with PBS supplemented with 3% FBS, followed by 1 hr incubation with ZIKV-specific HMAF (hyperimmune ascitic fluid). Plates were washed thrice followed by an hour-long incubation with a secondary antibody conjugated to horseradish peroxidase (KPL, Gaithersburg, MD). Detection proceeded with the addition of aminoethylcarbazole substrate (ENZO Life sciences, Farmingdale, NY) prepared according to the vendor's instructions.

SUPPLEMENTAL INFORMATION

Supplemental Information includes two figures, two tables, and Supplemental Experimental Procedures and can be found with this article at http://dx.doi.org/10.1016/j.chom.2016.05.004.

AUTHOR CONTRIBUTIONS

C.S., X.X., A.E.M., S.L.R., C.M.R., S.R.A., Y.Y., and N.B. conducted the experiments. C.S., X.X., R.B.T., N.B., A.D.B., N.V., S.C.W., and P.-Y.S. designed the experiments and wrote the paper.

ACKNOWLEDGMENTS

We are grateful to Mariano A. Garcia-Blanco, Shelton S. Brarick, and their lab members for providing lab space, equipment, and helpful discussions during the course of this work. We thank James C. Lee, Shirley J. Broz, Lisa M. Pipper, and Julia K. Melchor for their support during the establishment of P.-Y.S.'s lab at UTMB. This research was supported by NIH grants AI120942 and AI087856.

Received: April 14, 2016
Revised: May 4, 2016
Accepted: May 5, 2016
Published: May 16, 2016

REFERENCES

Alkan, C., Zapata, S., Bichaud, L., Moureau, G., Lemey, P., Firth, A.E., Gritsun, T.S., Gould, E.A., de Lamballerie, X., Depaquit, J., and Charrel, R.N. (2015). Ecuador Paraiso Escondido virus, a new flavivirus isolated from New World sand flies in Ecuador, Is the first representative of a novel clade in the genus flavivirus. J. Virol. *89*, 11773–11785.

Calvet, G., Aguiar, R.S., Melo, A.S., Sampaio, S.A., de Filippis, I., Fabri, A., Araujo, E.S., de Sequeira, P.C., de Mendonça, M.C., de Oliveira, L., et al. (2016). Detection and sequencing of Zika virus from amniotic fluid of fetuses with microcephaly in Brazil: a case study. Lancet Infect. Dis. S1473-3099(16)00095-5.

Chouin-Carneiro, T., Vega-Rua, A., Vazeille, M., Yebakima, A., Girod, R., Goindin, D., Dupont-Rouzeyrol, M., Lourenço-de-Oliveira, R., and Failloux, A.B. (2016). Differential Susceptibilities of Aedes aegypti and Aedes albopictus from the Americas to Zika virus. PLoS Negl. Trop. Dis. *10*, e0004543.

Dick, G.W., Kitchen, S.F., and Haddow, A.J. (1952). Zika virus. I. Isolations and serological specificity. Trans. R. Soc. Trop. Med. Hyg. *46*, 509–520.

Dudley, D.M., Aliota, M.T., Mohr, E.L., Weiler, A.M., Lehrer-Brey, G., Weisgrau, K.L., Mohns, M.S., Breitbach, M.E., Rasheed, M.N., Newman, C.M., et al. (2016). Natural history of Asian lineage Zika virus infection in macaques. bioRxiv. http://dx.doi.org/10.1101/046334.

Edmonds, J., van Grinsven, E., Prow, N., Bosco-Lauth, A., Brault, A.C., Bowen, R.A., Hall, R.A., and Khromykh, A.A. (2013). A novel bacterium-free method for generation of flavivirus infectious DNA by circular polymerase extension reaction allows accurate recapitulation of viral heterogeneity. J. Virol. *87*, 2367–2372.

Faria, N.R., Azevedo, Rdo.S., Kraemer, M.U., Souza, R., Cunha, M.S., Hill, S.C., Thézé, J., Bonsall, M.B., Bowden, T.A., Rissanen, I., et al. (2016). Zika virus in the Americas: early epidemiological and genetic findings. Science *352*, 345–349.

Fauci, A.S., and Morens, D.M. (2016). Zika virus in the Americas—yet another arbovirus threat. N. Engl. J. Med. *374*, 601–604.

Fitzpatrick, K.A., Deardorff, E.R., Pesko, K., Brackney, D.E., Zhang, B., Bedrick, E., Shi, P.Y., and Ebel, G.D. (2010). Population variation of West Nile virus confers a host-specific fitness benefit in mosquitoes. Virology *404*, 89–95.

Heang, V., Yasuda, C.Y., Sovann, L., Haddow, A.D., Travassos da Rosa, A.P., Tesh, R.B., and Kasper, M.R. (2012). Zika virus infection, Cambodia, 2010. Emerg. Infect. Dis. *18*, 349–351.

Khromykh, A.A., and Westaway, E.G. (1994). Completion of Kunjin virus RNA sequence and recovery of an infectious RNA transcribed from stably cloned full-length cDNA. J. Virol. *68*, 4580–4588.

Lai, C.J., Zhao, B.T., Hori, H., and Bray, M. (1991). Infectious RNA transcribed from stably cloned full-length cDNA of dengue type 4 virus. Proc. Natl. Acad. Sci. USA *88*, 5139–5143.

Lanciotti, R.S., Kosoy, O.L., Laven, J.J., Velez, J.O., Lambert, A.J., Johnson, A.J., Stanfield, S.M., and Duffy, M.R. (2008). Genetic and serologic properties of Zika virus associated with an epidemic, Yap State, Micronesia, 2007. Emerg. Infect. Dis. *14*, 1232–1239.

Lazear, H.M., Govero, J., Smith, A.M., Platt, D.J., Fernandez, E., Miner, J.J., and Diamond, M.S. (2016). A mouse model of Zika virus pathogenesis. Cell Host Microbe, Published online April 5, 2016. http://dx.doi.org/10.1016/j.chom.2016.03.010.

Li, S.H., Dong, H., Li, X.F., Xie, X., Zhao, H., Deng, Y.Q., Wang, X.Y., Ye, Q., Zhu, S.Y., Wang, H.J., et al. (2013). Rational design of a flavivirus vaccine by abolishing viral RNA 2′-O methylation. J. Virol. *87*, 5812–5819.

Li, X.D., Li, X.F., Ye, H.Q., Deng, C.L., Ye, Q., Shan, C., Shang, B.D., Xu, L.L., Li, S.H., Cao, S.B., et al. (2014). Recovery of a chemically synthesized Japanese encephalitis virus reveals two critical adaptive mutations in NS2B and NS4A. J. Gen. Virol. *95*, 806–815.

Lindenbach, B.D., Murray, C.J., Thiel, H.-J., and Rice, C.M. (2013). Flaviviridae. In Fields Virology, 6th, *Vol. 1*, D.M. Knipe and P.M. Howley, eds. (Philadelphia: Lippincott William & Wilkins), pp. 712–746.

Lo, M.K., Shi, P.Y., Chen, Y.L., Flint, M., and Spiropoulou, C.F. (2016). In vitro antiviral activity of adenosine analog NITD008 against tick-borne flaviviruses. Antiviral Res. *130*, 46–49.

Mandl, C.W., Ecker, M., Holzmann, H., Kunz, C., and Heinz, F.X. (1997). Infectious cDNA clones of tick-borne encephalitis virus European subtype prototypic strain Neudoerfl and high virulence strain Hypr. J. Gen. Virol. *78*, 1049–1057.

Mlakar, J., Korva, M., Tul, N., Popović, M., Poljšak-Prijatelj, M., Mraz, J., Kolenc, M., Resman Rus, K., Vesnaver Vipotnik, T., Fabjan Vodušek, V., et al. (2016). Zika virus associated with microcephaly. N. Engl. J. Med. *374*, 951–958.

Musso, D., Nhan, T., Robin, E., Roche, C., Bierlaire, D., Zisou, K., Shan Yan, A., Cao-Lormeau, V.M., and Broult, J. (2014). Potential for Zika virus transmission through blood transfusion demonstrated during an outbreak in French Polynesia, November 2013 to February 2014. Euro Surveill. *19*, http://dx.doi.org/10.2807/1560-7917.ES2014.19.14.20761.

Musso, D., Roche, C., Robin, E., Nhan, T., Teissier, A., and Cao-Lormeau, V.M. (2015). Potential sexual transmission of Zika virus. Emerg. Infect. Dis. *21*, 359–361.

Petersen, L.R., Jamieson, D.J., Powers, A.M., and Honein, M.A. (2016). Zika virus. N. Engl. J. Med. *374*, 1552–1563.

Rice, C.M., Grakoui, A., Galler, R., and Chambers, T.J. (1989). Transcription of infectious yellow fever RNA from full-length cDNA templates produced by in vitro ligation. New Biol. *1*, 285–296.

Rossi, S.L., Tesh, R.B., Azar, S.R., Muruato, A.E., Hanley, K.A., Auguste, A.J., Langsjoen, R.M., Paessler, S., Vasilakis, N., and Weaver, S.C. (2016). Characterization of a novel murine model to study Zika virus. Am. J. Trop. Med. Hyg. Published online March 28, 2016. http://dx.doi.org/10.4269/ajtmh.16-0111.

Shan, C., Xie, X., Barrett, A.D.T., Garcia-Blanco, M.A., Tesh, R.B., Vasconcelos, P.F.D.C., Vasilakis, N., Weaver, S.C., and Shi, P.Y. (2016). Zika virus: diagnosis, therapeutics, and vaccine. ACS Infectious Diseases *2*, 170–172.

Shi, P.Y., Tilgner, M., Lo, M.K., Kent, K.A., and Bernard, K.A. (2002). Infectious cDNA clone of the epidemic west nile virus from New York City. J. Virol. *76*, 5847–5856.

Shustov, A.V., Mason, P.W., and Frolov, I. (2007). Production of pseudoinfectious yellow fever virus with a two-component genome. J. Virol. *81*, 11737–11748.

Siridechadilok, B., Gomutsukhavadee, M., Sawaengpol, T., Sangiambut, S., Puttikhunt, C., Chin-inmanu, K., Suriyaphol, P., Malasit, P., Screaton, G., and Mongkolsapaya, J. (2013). A simplified positive-sense-RNA virus construction approach that enhances analysis throughput. J. Virol. *87*, 12667–12674.

Sumiyoshi, H., Hoke, C.H., and Trent, D.W. (1992). Infectious Japanese encephalitis virus RNA can be synthesized from in vitro-ligated cDNA templates. J. Virol. *66*, 5425–5431.

Tsetsarkin, K.A., and Weaver, S.C. (2011). Sequential adaptive mutations enhance efficient vector switching by Chikungunya virus and its epidemic emergence. PLoS Pathog. *7*, e1002412.

Tsetsarkin, K.A., Chen, R., Yun, R., Rossi, S.L., Plante, K.S., Guerbois, M., Forrester, N., Perng, G.C., Sreekumar, E., Leal, G., et al. (2014). Multi-peaked adaptive landscape for chikungunya virus evolution predicts continued fitness optimization in Aedes albopictus mosquitoes. Nat. Commun. *5*, 4084.

Wang, Q.Y., Patel, S.J., Vangrevelinghe, E., Xu, H.Y., Rao, R., Jaber, D., Schul, W., Gu, F., Heudi, O., Ma, N.L., et al. (2009). A small-molecule dengue virus entry inhibitor. Antimicrob. Agents Chemother. *53*, 1823–1831.

Whitehead, S.S., Blaney, J.E., Durbin, A.P., and Murphy, B.R. (2007). Prospects for a dengue virus vaccine. Nat. Rev. Microbiol. *5*, 518–528.

Yin, Z., Patel, S.J., Wang, W.L., Wang, G., Chan, W.L., Rao, K.R., Alam, J., Jeyaraj, D.A., Ngew, X., Patel, V., et al. (2006). Peptide inhibitors of Dengue virus NS3 protease. Part 1: Warhead. Bioorg. Med. Chem. Lett. *16*, 36–39.

Yin, Z., Chen, Y.L., Schul, W., Wang, Q.Y., Gu, F., Duraiswamy, J., Kondreddi, R.R., Niyomrattanakit, P., Lakshminarayana, S.B., Goh, A., et al. (2009). An adenosine nucleoside inhibitor of dengue virus. Proc. Natl. Acad. Sci. USA *106*, 20435–20439.

Zmurko, J., Marques, R.E., Schols, D., Verbeken, E., Kaptein, S.J.F., and Neyts, J. (2016). The viral polymerase inhibitor 7-deaza-2′-C-methyladenosine is a potent inhibitor of in vitro Zika virus replication and delays disease progression in a robust mouse infection model. bioRxiv. http://dx.doi.org/10.1101/041905.

Zou, G., Xu, H.Y., Qing, M., Wang, Q.Y., and Shi, P.Y. (2011). Development and characterization of a stable luciferase dengue virus for high-throughput screening. Antiviral Res. *91*, 11–19.

Züst, R., Dong, H., Li, X.F., Chang, D.C., Zhang, B., Balakrishnan, T., Toh, Y.X., Jiang, T., Li, S.H., Deng, Y.Q., et al. (2013). Rational design of a live attenuated dengue vaccine: 2′-o-methyltransferase mutants are highly attenuated and immunogenic in mice and macaques. PLoS Pathog. *9*, e1003521.